A&A 588, L4 (2016)
DOI: 10.1051/0004-6361/201628261

Astronomy & Astrophysics

Letter to the Editor

Discovery of a massive supercluster system at $z \sim 0.47$

H. Lietzen[1,2], E. Tempel[3], L. J. Liivamägi[3], A. Montero-Dorta[4], M. Einasto[3], A. Streblyanska[1,2], C. Maraston[5], J. A. Rubiño-Martín[1,2], and E. Saar[3]

[1] Instituto de Astrofísica de Canarias, 38200 La Laguna, Tenerife, Spain
e-mail: heidi.lietzen@gmail.com
[2] Universidad de La Laguna, Dept. Astrofísica, 38206 La Laguna, Tenerife, Spain
[3] Tartu Observatory, Observatooriumi 1, 61602 Tõravere, Estonia
[4] Department of Physics and Astronomy, The University of Utah, 115 South 1400 East, Salt Lake City, UT 84112, USA
[5] ICG-University of Portsmouth, Dennis Sciama Building, Burnaby Road, PO1 3FX, Portsmouth, UK

Received 5 February 2016 / Accepted 24 February 2016

ABSTRACT

Aims. Superclusters are the largest relatively isolated systems in the cosmic web. Using the SDSS BOSS survey, we search for the largest superclusters in the redshift range $0.43 < z < 0.71$.
Methods. We generate a luminosity-density field smoothed over 8 h^{-1}Mpc to detect the large-scale over-density regions. Each individual over-density region is defined as single supercluster in the survey. We define the superclusters so that they are comparable to the superclusters found in the SDSS main survey.
Results. We find a system that we call the BOSS Great Wall (BGW), which consists of two walls with diameters 186 and 173 h^{-1} Mpc and two other major superclusters with diameters of 64 and 91 h^{-1} Mpc. As a whole, this system consists of 830 galaxies with the mean redshift 0.47. We estimate the total mass to be approximately $2 \times 10^{17}\ h^{-1}\ M_{\odot}$. The morphology of the superclusters in the BGW system is similar to the morphology of the superclusters in the Sloan Great Wall region.
Conclusions. The BGW is one of the most extended and massive systems of superclusters found so far in the Universe.

Key words. large-scale structure of Universe

1. Introduction

The large-scale structure of the Universe can be seen as the cosmic web of clusters and groups of galaxies connected by filaments, with under-dense voids between the over-dense regions (Bond et al. 1996). The largest over-dense, relatively isolated systems in the cosmic web are the superclusters of galaxies (de Vaucouleurs 1956; Jõeveer et al. 1978; Zucca et al. 1993; Einasto et al. 1994).

Several supercluster catalogs have been compiled recently (Einasto et al. 2007; Liivamägi et al. 2012; Chow-Martínez et al. 2014; Nadathur & Hotchkiss 2014), providing material for studies of the large-scale structure. We are now extending the knowledge of superclusters to the redshifts above 0.45, using the constant mass (CMASS) sample of the Sloan Digital Sky Survey III (SDSS-III; Eisenstein et al. 2011; Maraston et al. 2013; Reid et al. 2016). Only a few relatively small superclusters have been found at high redshifts before (Tanaka et al. 2007; Schirmer et al. 2011; Pompei et al. 2016).

We have found an unusually extended overdensity within the SDSS/CMASS volume at redshift $z \sim 0.47$. This structure resembles the Sloan Great Wall, which consists of several superclusters and is the richest and largest system found in the nearby universe (Vogeley et al. 2004; Einasto et al. 2011b). Another comparison point is the local Laniakea supercluster with a 160 Mpc diameter (Tully et al. 2014; Tempel 2014).

Throughout this paper, we assume a ΛCDM cosmology with total matter density $\Omega_{\rm m} = 0.27$, dark energy density $\Omega_{\Lambda} = 0.73$. We express the Hubble constant as $H_0 = 100\,h\,{\rm km\,s^{-1}\,Mpc^{-1}}$(Komatsu et al. 2011).

2. Data

We used data from the twelfth data release (DR12) of the SDSS (Alam et al. 2015; York et al. 2000) Baryon Oscillation Spectroscopic Survey (BOSS; Eisenstein et al. 2011; Bolton et al. 2012; Dawson et al. 2013). We used the CMASS sample, which targets galaxies in the redshift range $0.43 < z < 0.7$. The BOSS data is obtained using a multi-object spectrograph (Smee et al. 2013) on the 2.5-m telescope (Gunn et al. 2006) located at Apache Point Observatory in New Mexico. The SDSS imaging was done with a drift-scanning mosaic CCD camera (Gunn et al. 1998) in five color-bands, u, g, r, i, z (Fukugita et al. 1996), and it was published in data release 8 (DR8; Aihara et al. 2011). BOSS obtains spectra with resolutions of 1500 to 2600 in the wavelength range 3600 to 10 000 Å (Smee et al. 2013).

The CMASS sample selects massive and luminous galaxies at redshift above $z \sim 0.4$, whose stellar mass remains approximately constant up to $z \sim 0.6$. In principle, the selection criteria allow the detection of galaxies with arbitrary colors, because the CMASS cut does not impose any limit on the observed-frame $g - r$. In practice, the CMASS cut selects the massive end of the red sequence, since these are the most abundant galaxies at the high mass end ($M > 10^{11}\ M_{\odot}$), and they do not evolve over the CMASS redshift range. The CMASS sample was selected to isolate the massive end of the red sequence at $z \sim 0.5$. First, a preselection was performed to ensure that the targets pass a set of quality criteria described in Dawson et al. (2013). The final selection was made based on the observed colors and magnitudes (Cannon et al. 2006; Abazajian et al. 2009; Anderson et al. 2012).

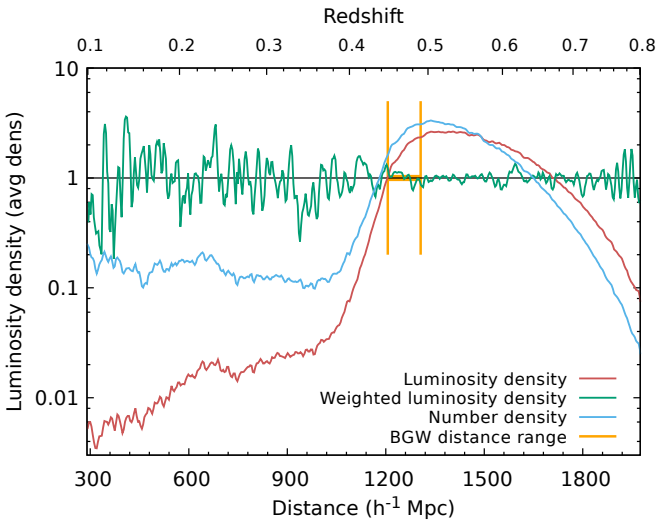

Fig. 1. Number density (blue), luminosity density (red), and weighted luminosity density (green) of the CMASS galaxies as a function of distance. The densities are given in units of mean density. The orange region shows the discovered BGW region.

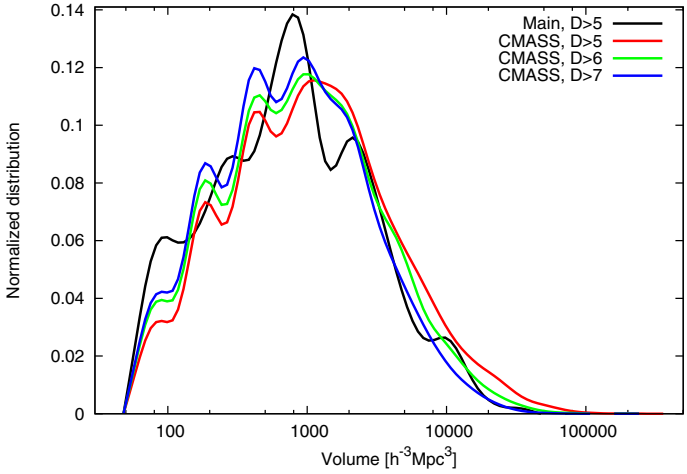

Fig. 2. Distribution of supercluster volumes. For comparison, the distribution of the SDSS DR7 main sample is shown with the black curve. The CMASS supercluster volume distribution is shown for three density thresholds (in units of mean density): $D > 5$ (red), $D > 6$ (green), and $D > 7$ (blue).

For a comparison to the low-redshift universe, we used the SDSS DR7 main sample superclusters from Liivamägi et al. (2012). This sample consists of 583 362 galaxies in a volume of $1.32 \times 10^8\,h^{-3}\,\mathrm{Mpc}^3$ with mean number density $4.4 \times 10^{-3}\,h^3\,\mathrm{Mpc}^{-3}$. The comparison sample includes nearly 1000 superclusters.

3. Methods

We constructed a luminosity-density field to distinguish the superclusters from the lower-density regions following the same procedure as was used in Liivamägi et al. (2012). We weighted the luminosities of galaxies to set the mean density to be the same throughout the distance range, and then calculated the density field in a $3\,h^{-1}$ Mpc grid with an $8\,h^{-1}$ Mpc smoothing scale.

The number density and the luminosity density of the galaxies vary with distance as shown in Fig. 1. The weighting suppresses this variation, making the mean luminosity density remain constant with small random variation throughout the distance range from 1200 to $1800\,h^{-1}$ Mpc. We also trimmed the edges of the sample in the survey coordinates with the limits $-50.0° < \lambda < 51.5°$, $-34.5° < \eta < 36.25°$, where λ and η are the SDSS survey coordinates. In the SDSS, the survey coordinates form a spherical coordinate system, where $(\eta, \lambda) = (0, 90.)$ corresponds to $(\mathrm{RA}, \mathrm{Dec}) = (275., 0.)$ and $(\eta, \lambda) = (57.5, 0.)$ corresponds to $(\mathrm{RA}, \mathrm{Dec}) = (0., 90.)$. At $(\eta, \lambda) = (0., 0.)$, $(\mathrm{RA}, \mathrm{Dec}) = (185., 32.5)$. The volume of the luminosity-density field with these limits is $2.62 \times 10^9\,h^{-3}\,\mathrm{Mpc}^3$, and it contains 480 801 galaxies, making the mean number density of galaxies $1.8 \times 10^{-4}\,h^3\,\mathrm{Mpc}^{-3}$.

In previous studies of the SDSS main sample, the threshold density of 5.0 times the mean density has often been used as the limit for superclusters (e.g., Tempel et al. 2011; Lietzen et al. 2012; Einasto et al. 2014). We used the main sample superclusters from Liivamägi et al. (2012) as a comparison to the superclusters in the CMASS sample. Figure 2 shows the volume distribution for superclusters found with density thresholds of five, six, and seven mean densities compared to the SDSS main sample in DR7 with density threshold of five times the mean density. The volume was calculated as the number of grid cells multiplied by the volume of one cell. Since the grid size in the CMASS density field is $3\,h^{-1}$ Mpc, the volume of a grid cell is $27\,(h^{-1}\mathrm{Mpc})^3$ [1]. The distributions of supercluster volumes with these three thresholds are close to those of the main-sample superclusters, suggesting that the density limit to determine superclusters should be around these density levels.

4. Results

The largest structure that we found with the density threshold $D > 5$ mean densities has a diameter of $271\,h^{-1}$ Mpc and a volume of $2.4 \times 10^5 (h^{-1}\mathrm{Mpc})^3$, and it contains 830 galaxies. The richness difference to the other structures is significant, since the second richest one only contains 390 galaxies. The structure of the largest system is more complex than the structure of the SDSS main sample superclusters, which contain several separate cores. This suggests that structures found with this density threshold are not individual superclusters, but systems of several separate superclusters. This system can be seen as comparable to the Sloan Great Wall, which is also a system of several superclusters (Einasto et al. 2011b).

When we increase the density threshold, the unusually high overdensity found with $D > 5$ level breaks down in several parts. With the density level $D > 6$ mean densities, the individual superclusters can be distinguished from each other. The structure is shown in sky coordinates in Fig. 3, with the galaxies in the four largest superclusters shown with filled symbols, and the other galaxies belonging to the $D > 5$ overdensity shown with crosses. The most prominent feature of the structure are two walls with diameters $186\,h^{-1}$ Mpc (supercluster A in Fig. 3) and $173\,h^{-1}$ Mpc (supercluster B in Fig. 3). Again, these are the two largest superclusters in the whole sample according to diameter. In addition, there are two moderately large superclusters (labeled C and D in Fig. 3) with diameters 64 and $91\,h^{-1}$ Mpc and a few small superclusters with less than 15 galaxies within this structure.

[1] The grid size of the main SDSS sample field is $1\,h^{-1}$ Mpc. Since we smooth the density field in both the SDSS and CMASS samples with an $8\,h^{-1}$ Mpc kernel, the grid size of $3\,h^{-1}$ Mpc is equally comparable to the grid size of $1\,h^{-1}$ Mpc.

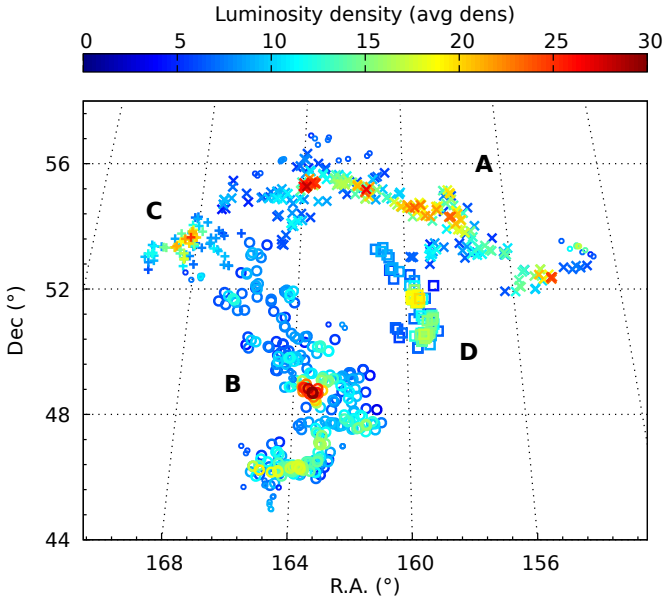

Fig. 3. Galaxies in the BOSS Great Wall (BGW) in sky coordinates. The color scale shows the local environmental density in terms of mean densities for each galaxy. The different symbols refer to galaxies in the four largest superclusters in the system determined with the density threshold $D > 6$.

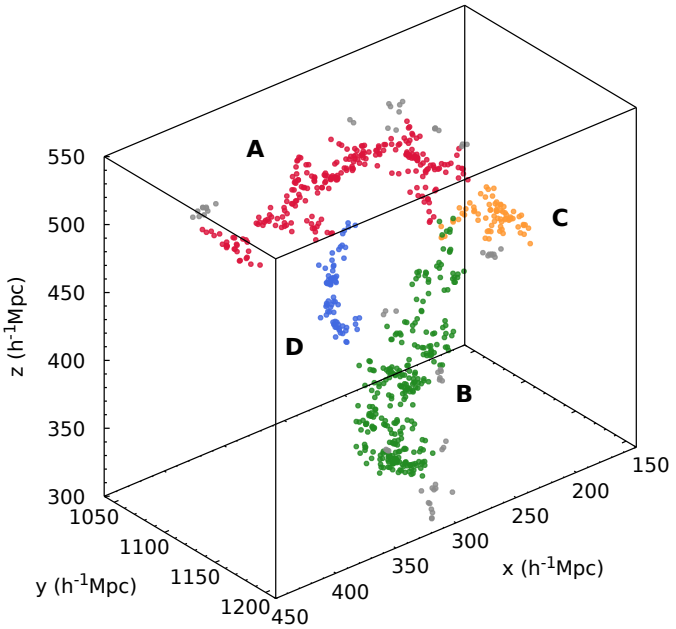

Fig. 4. Galaxies in the BGW superclusters in Cartesian coordinates. Different colors show the individual superclusters in the BGW system.

We analyzed the shapes of the two richest superclusters A and B using the shape parameter K that is defined with Minkowski functionals (see Einasto et al. 2011a, for details). This is the ratio of two parameters, planarity and filamentarity, which both may change from 0 to 1 (from a sphere to a plane or to a line). The smaller the parameter, the more elongated a system is. The superclusters A and B are very elongated, with the shape parameter values 0.17 and 0.19. For a comparison, the richest supercluster in the Sloan Great Wall has the shape parameter $K = 0.27$, and is therefore less elongated than these two superclusters.

In Fig. 4 the supercluster galaxies are shown in the three-dimensional Cartesian coordinates which were defined as

$$x = -d \sin \lambda \quad (1)$$

$$y = d \cos \lambda \cos \eta \quad (2)$$

$$z = d \cos \lambda \sin \eta, \quad (3)$$

where d is the distance of the galaxy and η and λ are the SDSS angular coordinates. The basic information about the two walls and the two companion superclusters is given in Table 1. We present an interactive 3D model showing the distribution of galaxies in the BGW[2].

4.1. Total mass of the BGW superclusters

We used stellar masses to estimate a minimum mass for the BGW and its member superclusters. BOSS stellar masses are obtained from the Portsmouth galaxy product (Maraston et al. 2013), which is based on the stellar population models of Maraston (2005) and Maraston et al. (2009). The Portsmouth product uses an adaptation of the publicly-available Hyper-Z code (Bolzonella et al. 2000) to perform a best-fit to the observed *ugriz* magnitudes of BOSS galaxies, with the spectroscopic redshift determined by the BOSS pipeline. The stellar masses that we use in this work were computed assuming a Kroupa initial mass function.

Stellar masses of galaxies in superclusters are typically higher than at low densities (Einasto et al. 2014). Similarly, in the BGW system, the stellar masses of galaxies in the two walls are higher than the stellar masses in a control sample of galaxies with the local density level $D < 2$ times the mean density with median values 9.1×10^{10} for supercluster A, 8.3×10^{10} for supercluster B, and 6.9×10^{10} for the low-density galaxies. According to the Kolmogorov-Smirnov (KS) test, both walls have a stellar mass distribution that differs from the low-density galaxies to a very high level of significance: p-values are less than 10^{-10}. For the difference between the two walls, the KS test gives the p-value of 0.0329, which means that the stellar mass distributions are different when the significance level is 95%.

We estimate a lower limit for the mass of the walls using the stellar mass M_* to halo mass $M_{\rm halo}$ relation as given by Moster et al. (2010), assuming that all galaxies in the CMASS sample are central galaxies of a halo. According to Maraston et al. (2013), the sample is roughly complete at stellar masses above $10^{11.3}\ h^{-1}\ M_\odot$ in our redshift range (see also Leauthaud et al. 2016). The sample therefore misses the halos that only host low-mass galaxies because of the data selection. We correct for this incompleteness by scaling the SDSS main sample of galaxies as a comparison. For this we used the magnitude-limited galaxy and friend-of-friend (FoF) group catalog by Tempel et al. (2014) in the distance bin from 180 to 270 h^{-1} Mpc. In this sample, the ratio between stellar mass in BOSS-like sample of galaxies with $\log(M_*/h^{-1}M_\odot) > 11.3$ and the most luminous galaxies of the FoF groups in superclusters is 0.082. Correcting the mass in the BGW superclusters with this ratio, we get masses $5.9 \times 10^{16}\ h^{-1}\ M_\odot$ for supercluster A, $4.4 \times 10^{16}\ h^{-1}\ M_\odot$ for supercluster B, and $1.6 \times 10^{17}\ h^{-1}\ M_\odot$ for the whole system.

Another way to estimate the total mass of the superclusters is to use the critical density of the Universe ρ_c. We assumed that mass density correlates with luminosity density and calculated the mass of each grid cell belonging to the superclusters as $M = \rho_c D V$, where D is the luminosity density in the units of mean

[2] http://www.aai.ee/~maret/BOSSWalls.html

Table 1. Basic information on the main superclusters in the BGW supercluster system and the whole system.

Supercluster	Richness N_{gal}	Diameter h^{-1} Mpc	Volume $(h^{-1}$ Mpc$)^3$	Average density $\langle\rho_L\rangle$	Maximum density $\langle\rho_L\rangle$	$\log(M_1)$ $\log(h^{-1}M_\odot)$	$\log(M_2)$ $\log(h^{-1}M_\odot)$
A	255	186.1	67500	9.1	27.9	16.8	16.9
B	303	172.9	70848	9.3	29.6	16.6	16.9
C	73	63.8	19008	10.2	24.5	16.3	16.4
D	71	90.6	13635	9.3	21.2	16.0	16.2
Total	830	271.1	241029	8.6	29.6	17.2	17.4

Notes. The line "Total" refers to the over-dense region found with the threshold of $D > 5$ mean densities. The individual superclusters in the BGW are found with the threshold $D > 6$. The two mass estimates are the mass derived from the stellar masses ($\log(M_1)$) and the mass derived from the critical density ($\log(M_2)$).

densities, and $V = 27\ h^{-3}$ Mpc^3 is the volume of the cell. With this method we get masses $8.2 \times 10^{16}\ h^{-1}\ M_\odot$ for supercluster A and $7.7 \times 10^{16}\ h^{-1}\ M_\odot$ for supercluster B. The mass of the BGW in total is $2.4 \times 10^{17}\ h^{-1}\ M_\odot$. The mass estimates for all BGW superclusters are shown in Table 1.

5. Discussion and conclusions

We found two walls of galaxies at redshift $0.45 < z < 0.5$ that are larger in volume and diameter than any previously known superclusters. Together they form the system of the BOSS Great Wall, which is more extended than any other known structure. The closest comparison to this system is the Sloan Great Wall, which is also a system of several large superclusters and complexes of superclusters connected with the Sloan Great Wall (Einasto et al. 2011a). However, the volume of the main supercluster of the Sloan Great Wall is $2.5 \times 10^4\ (h^{-1}$ Mpc$)^3$, which is smaller than the volumes of either of the walls in the BGW (Einasto et al. 2011b). The BGW system as a whole covers a volume of $2.4{\times}10^5\ (h^{-1}$ Mpc$)^3$ of which $1.7{\times}10^5\ (h^{-1}$ Mpc$)^3$ consists of the four largest superclusters. With the diameter of 271 h^{-1} Mpc, the BGW is considerably more extended than the Sloan Great Wall, which has a diameter of approximately $160\,h^{-1}$ Mpc (Sheth & Diaferio 2011), or the local Laniakea supercluster, whose full basin of attraction has a diameter of 160 Mpc (Tully et al. 2014).

Stellar masses have not been used previously to estimate the total masses of superclusters. Our mass estimates from stellar masses agree well with our estimate from critical density. Our analysis suggests that both of the walls in the BGW are comparable to the entire Sloan Great Wall, whose mass is estimated to be within 20% of $1.2 \times 10^{17}\ h^{-1}\ M_\odot$ (Sheth & Diaferio 2011). We can therefore conclude that the total mass of the BGW system is approximately $2{\times}10^{17}\ h^{-1}\ M_\odot$, making the BGW the most massive system of superclusters found in the Universe.

Acknowledgements. The authors thank Brent Tully for his valuable suggestions for improving the article as a referee. H.L., A.S., and J.A.R.-M. acknowledge financial support from the Spanish Ministry of Economy and Competitiveness (MINECO) under the 2011 Severo Ochoa Program MINECO SEV-2011-0187. E.T., L.J.L., M.E., and E.S. were supported by the ETAG projects IUT26-2, IUT40-2, and TK133. A.M.D. acknowledges support from the US Department of Energy, Office of Science, Office of High Energy Physics, under Award Number DE-SC0010331. A.M.D. also thanks the Center for High Performance Computing at the University of Utah for its support and resources. Funding for SDSS-III has been provided by the Alfred P. Sloan Foundation, the Participating Institutions, the National Science Foundation, and the US Department of Energy Office of Science. The SDSS-III web site is http://www.sdss3.org/. SDSS-III is managed by the Astrophysical Research Consortium for the Participating Institutions of the SDSS-III Collaboration including the University of Arizona, the Brazilian Participation Group, Brookhaven National Laboratory, Carnegie Mellon University, University of Florida, the French Participation Group, the German Participation Group, Harvard University, the Instituto de Astrofisica de Canarias, the Michigan State/Notre Dame/JINA Participation Group, Johns Hopkins University, Lawrence Berkeley National Laboratory, Max Planck Institute for Astrophysics, Max Planck Institute for Extraterrestrial Physics, New Mexico State University, New York University, Ohio State University, Pennsylvania State University, University of Portsmouth, Princeton University, the Spanish Participation Group, University of Tokyo, University of Utah, Vanderbilt University, University of Virginia, University of Washington, and Yale University.

References

Abazajian, K. N., Adelman-McCarthy, J. K., Agüeros, M. A., et al. 2009, ApJS, 182, 543
Aihara, H., Allende Prieto, C., An, D., et al. 2011, ApJS, 193, 29
Alam, S., Albareti, F. D., Allende Prieto, C., et al. 2015, ApJS, 219, 12
Anderson, L., Aubourg, E., Bailey, S., et al. 2012, MNRAS, 427, 3435
Bolton, A. S., Schlegel, D. J., Aubourg, É., et al. 2012, AJ, 144, 144
Bolzonella, M., Miralles, J.-M., & Pelló, R. 2000, A&A, 363, 476
Bond, J. R., Kofman, L., & Pogosyan, D. 1996, Nature, 380, 603
Cannon, R., Drinkwater, M., Edge, A., et al. 2006, MNRAS, 372, 425
Chow-Martínez, M., Andernach, H., Caretta, C. A., & Trejo-Alonso, J. J. 2014, MNRAS, 445, 4073
Dawson, K. S., Schlegel, D. J., Ahn, C. P., et al. 2013, AJ, 145, 10
de Vaucouleurs, G. 1956, Vistas Astron., 2, 1584
Einasto, M., Einasto, J., Tago, E., Dalton, G. B., & Andernach, H. 1994, MNRAS, 269, 301
Einasto, J., Einasto, M., Tago, E., et al. 2007, A&A, 462, 811
Einasto, M., Liivamägi, L. J., Tago, E., et al. 2011a, A&A, 532, A5
Einasto, M., Liivamägi, L. J., Tempel, E., et al. 2011b, ApJ, 736, 51
Einasto, M., Lietzen, H., Tempel, E., et al. 2014, A&A, 562, A87
Eisenstein, D. J., Weinberg, D. H., Agol, E., et al. 2011, AJ, 142, 72
Fukugita, M., Ichikawa, T., Gunn, J. E., et al. 1996, AJ, 111, 1748
Gunn, J. E., Carr, M., Rockosi, C., et al. 1998, AJ, 116, 3040
Gunn, J. E., Siegmund, W. A., Mannery, E. J., et al. 2006, AJ, 131, 2332
Jõeveer, M., Einasto, J., & Tago, E. 1978, MNRAS, 185, 357
Komatsu, E., Smith, K. M., Dunkley, J., et al. 2011, ApJS, 192, 18
Leauthaud, A., Bundy, K., Saito, S., et al. 2016, MNRAS, 457, 4021
Lietzen, H., Tempel, E., Heinämäki, P., et al. 2012, A&A, 545, A104
Liivamägi, L. J., Tempel, E., & Saar, E. 2012, A&A, 539, A80
Maraston, C. 2005, MNRAS, 362, 799
Maraston, C., Strömbäck, G., Thomas, D., Wake, D. A., & Nichol, R. C. 2009, MNRAS, 394, L107
Maraston, C., Pforr, J., Henriques, B. M., et al. 2013, MNRAS, 435, 2764
Moster, B. P., Somerville, R. S., Maulbetsch, C., et al. 2010, ApJ, 710, 903
Nadathur, S., & Hotchkiss, S. 2014, MNRAS, 440, 1248
Pompei, E., Adami, C., Eckert, D., et al. 2016, A&A, in press, DOI: 10.1051/0004-6361/201527142
Reid, B., Ho, S., Padmanabhan, N., et al. 2016, MNRAS, 455, 1553
Schirmer, M., Hildebrandt, H., Kuijken, K., & Erben, T. 2011, A&A, 532, A57
Sheth, R. K., & Diaferio, A. 2011, MNRAS, 417, 2938
Smee, S. A., Gunn, J. E., Uomoto, A., et al. 2013, AJ, 146, 32
Tanaka, M., Hoshi, T., Kodama, T., & Kashikawa, N. 2007, MNRAS, 379, 1546
Tempel, E. 2014, Nature, 513, 41
Tempel, E., Saar, E., Liivamägi, L. J., et al. 2011, A&A, 529, A53
Tempel, E., Tamm, A., Gramann, M., et al. 2014, A&A, 566, A1
Tully, R. B., Courtois, H., Hoffman, Y., & Pomarède, D. 2014, Nature, 513, 71
Vogeley, M. S., Hoyle, F., Rojas, R. R., & Goldberg, D. M. 2004, in IAU Colloq. 195: Outskirts of Galaxy Clusters: Intense Life in the Suburbs, ed. A. Diaferio, 5
York, D. G., Adelman, J., Anderson, Jr., J. E., et al. 2000, AJ, 120, 1579
Zucca, E., Zamorani, G., Scaramella, R., & Vettolani, G. 1993, ApJ, 407, 470